Controlled-PHASE Gate for Photons Based on Stationary Light

Ivan Iakoupov,[1] Johannes Borregaard,[1,2] and Anders S. Sørensen[1]
[1]The Niels Bohr Institute, University of Copenhagen, Blegdamsvej 17, DK-2100 Copenhagen Ø, Denmark
[2]Department of Physics, Harvard University, Cambridge, Massachusetts 02138, USA

(Received 2 November 2016; revised manuscript received 31 October 2017; published 4 January 2018)

We propose a method to induce strong effective interactions between photons mediated by an atomic ensemble. To achieve this, we use the so-called stationary light effect to enhance the interaction. Regardless of the single-atom coupling to light, the interaction strength between the photons can be enhanced by increasing the total number of atoms. For sufficiently many atoms, the setup can be viable as a controlled-PHASE gate for photons. We derive analytical expressions for the fidelities for two modes of gate operation: deterministic and heralded conditioned on the presence of two photons at the output.

DOI: 10.1103/PhysRevLett.120.010502

Optical photons are ideal carriers of quantum information over long distances, and such quantum communication may enable a wealth of applications [1]. Quantum information processing with photonic qubits is, however, severely limited by the lack of efficient two-qubit gates. In principle, such gates could be realized by strongly coupling photons to a single atom [2,3]. Experiments have pushed towards realizing such strong coupling, e.g., in cavity QED structures [4–8] and optical waveguides [9–12], but the realization of two-qubit gates remains challenging. For some applications, it is possible to use atomic ensembles where a large number of atoms compensates for a weak single-atom coupling strength [13]. However, this approach typically does not enhance the nonlinear interactions required for quantum gates. Gate operation is often pursued by extending the ensemble approach with strong dipole-dipole interactions of the atomic Rydberg levels [14–19]. In recent years, experiments in, e.g., tapered optical fibers [20–24] and hollow core photonic-crystal fibers [25,26] have realized an intermediate regime where the single-atom coupling to light is sizable, but still not sufficient to realize photonic gates based on single atoms. It remains an open question to which degree such moderate couplings enable processing of quantum information.

In this Letter, we propose a controlled-PHASE gate that works even if the individual atoms are not coupled strongly either to light (e.g., optical cavities) or to each other (e.g., Rydberg interactions). We show that by using sufficiently many atoms, it is possible to compensate for the limited single-atom coupling to light and achieve ideal gate operation [27]. The main physical mechanism behind the gate is *stationary light* [28,29] where polaritons (coupled light-matter excitations) have very low group velocity due to counterpropagating classical drives. These polaritons experience reflections at the ends of the ensemble. This leads to transmission resonances whenever the polaritons form standing waves inside the ensemble [27], akin to an optical cavity. We show that the storage of a single photon completely changes the scattering properties of the ensemble because the cavitylike structure created by the remaining atoms enhances the interaction with the stored excitation. This can be used to mediate a gate between photons that can be either deterministic or heralded (successful operation is conditioned on subsequent detection of two photons).

Overview.—We consider two different level schemes for the atoms in the ensemble: Λ-type and dual-V [Figs. 1(a) and 1(b), respectively]. The linear properties of these two schemes are described in detail in Ref. [30]. In the Λ-type scheme, two counterpropagating classical drives have the same polarization and frequency. This results in a standing wave of the Rabi frequency $\Omega(z) = \Omega_0 \cos(k_0 z)$, where k_0 is the wave vector of the classical drive, assumed to be the same as the wave vector of the probe field $\hat{\mathcal{E}}$ (single photon). For the Λ-type scheme, we assume that N atoms are placed at positions $z_j = j\pi/(2k_0)$ with $0 \leq j \leq N-1$ to achieve the lowest possible group velocity (increasing the interatomic distance by integer multiples of π/k_0 does not change the results) [30]. Low group velocity can also be achieved by separating the two counterpropagating classical drives either in polarization [31] or frequency [32]. We choose the separation in polarization, i.e., the dual-V scheme, but separation in frequency is expected to yield similar results [30]. From a practical perspective, the dual-V scheme is desirable since it does not require careful placement of the atoms. However, we focus on the Λ-type scheme in the analysis below, since it admits an approximate analytical solution. We also perform the numerical analysis for both of the schemes and show that the analytical results obtained for the Λ-type scheme provide the correct scaling for the dual-V scheme.

The single-atom coupling to light is characterized by the parameter Γ_{1D}/Γ (half of the resonant optical depth per atom), where Γ_{1D} is the decay rate from each of the states

 © 2018 American Physical Society

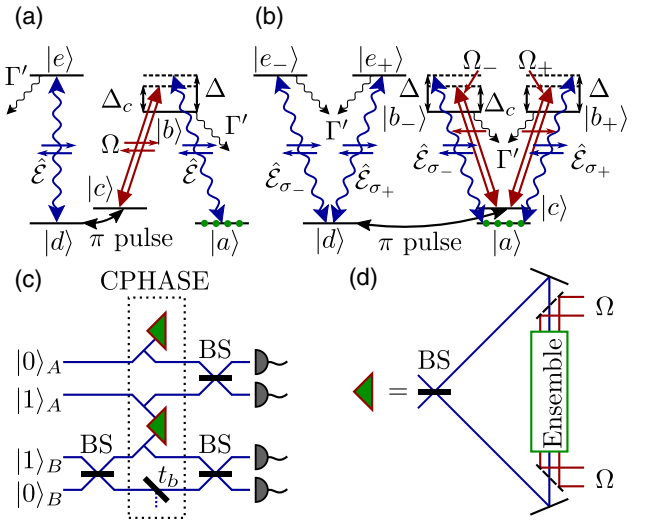

FIG. 1. (a) Level diagram of Λ-type atoms (levels $|a\rangle$, $|b\rangle$, and $|c\rangle$) that can be switched to two-level atoms (levels $|d\rangle$ and $|e\rangle$) by the storage of a photon followed by a π pulse. Green dots indicate the initial state of the atoms. (b) Level diagram of dual-V atoms that can be switched to V-type atoms. (c) Dual-rail Bell-state measurement setup with the controlled-PHASE (CPHASE) gate as a part of it. An ensemble of atoms is placed inside a Sagnac interferometer, shown as a triangle in (c) and defined by (d). In the rail corresponding to state $|0\rangle_B$, a beam splitter is added with transmission coefficient t_b. All the other beam splitters (BS) are 50:50.

$|b\rangle$ and $|e\rangle$ [see Fig. 1(a)] into both right-moving and left-moving guided modes (assumed to be equal), Γ' is the decay rate into all the other modes, and $\Gamma = \Gamma_{1D} + \Gamma'$ is the total decay rate. In the dual-rail encoding of photonic qubits shown in Fig. 1(c), two identical atomic ensembles are required, where the upper one only functions as a memory. Alternatively, the single-rail encoding can also be implemented with one atomic ensemble [18], but the dual-rail encoding allows heralded operation that has better fidelity. Each ensemble is placed inside a Sagnac interferometer [Fig. 1(d)].

The operation of the CPHASE gate is sequential. First, photon A is stored either in the upper ($|0\rangle_A$) or the lower ($|1\rangle_A$) ensemble using electromagnetically induced transparency (EIT) [33]. Then photon B is scattered from the lower ensemble under stationary light conditions ($|1\rangle_B$) or passes through a beam splitter with transmission coefficient t_b ($|0\rangle_B$). The role of this beam splitter will be explained below. The Sagnac interferometer can be set up such that most of the incident power in each of its two input ports is reflected back through the same port, regardless of whether the ensemble is reflective or transmissive [34,35]. Reflection or transmission of the ensemble instead controls the phase of the reflected field. The scattering of photon B can be arranged such that if there is no stored photon in the lower ensemble (photon A is in the state $|0\rangle_A$), the atomic ensemble is completely transmissive in the ideal case, and photon B is reflected from the Sagnac interferometer with no additional phase. If there is a stored photon (photon A is in state $|1\rangle_A$), photon B is reflected from the interferometer with a π phase shift. The latter case performs the desired CPHASE gate operation $|11\rangle_{AB} \to -|11\rangle_{AB}$, while the rest of the basis states are unchanged. Finally, photon A is retrieved using EIT.

Storage and retrieval.—Before the EIT storage, all atoms are initialized in state $|a\rangle$, and after storage, the incident photon is mapped onto an atom being in state $|c\rangle$. To produce an optical nonlinearity, we assume that state $|c\rangle$ is subsequently transferred to state $|d\rangle$ using a π pulse. Under EIT storage and retrieval, both the incident photon and the classical drive are assumed resonant with the respective atomic transitions for simplicity. The classical drive is incident from one side only. Entering the Sagnac interferometer, photon A is split into two parts by the 50:50 beam splitter [see Fig. 1(d)]. The two parts reach the ensemble from the opposite sides with opposite spatial phase factors $e^{ik_0 z}$ and $e^{-ik_0 z}$. Inside the ensemble, the two parts will interfere, resulting in a stored spin wave with $\cos(k_0 z)$ spatial modulation. Such storage procedure is necessary (for the Λ-type scheme only), since the part of the excitation that is stored on the nodes of the standing wave of the classical drive (that is applied during scattering of photon B) does not change the scattering properties of the ensemble.

Reflection and transmission.—We use the (multimode) transfer matrix formalism [30,36] to model the scattering process. To illustrate the scattering behavior, we assume that photon A was stored in the center of the atomic ensemble at an antinode of the classical drive. The reflectances and transmittances of an ensemble of Λ-type atoms are plotted in Fig. 2 as functions of the two-photon detuning $\delta = \Delta - \Delta_c$, where Δ (Δ_c) is the detuning of the probe field (classical drive). The reflectance $|r_0|^2$ ($|r_1|^2$) and transmittance $|t_0|^2$ ($|t_1|^2$) are for an ensemble without (with) a stored photon. The ensemble is seen to have transmittance resonances with a large $|t_0|^2$ and a small $|r_0|^2$. These resonances occur when the standing wave condition is

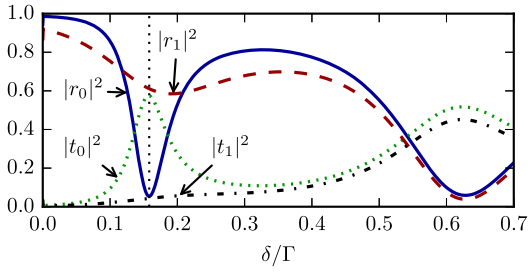

FIG. 2. (a) Reflectances ($|r_0|^2$, $|r_1|^2$) and transmittances ($|t_0|^2$, $|t_1|^2$) of an ensemble of Λ-type atoms without ($|r_0|^2$, $|t_0|^2$) and with ($|r_1|^2$, $|t_1|^2$) a stored photon for different frequencies (two-photon detunings) δ. The vertical dotted line marks the operation point δ_{res}. The parameters are $N = 10^4$, $\Gamma_{1D}/\Gamma = 0.05$, $\Delta_c/\Gamma = -10$, and $\Omega_0/\Gamma = 10$.

fulfilled, i.e., $\sin(qL) = 0$, where q is the Bloch vector of the stationary light polaritons and L is the length of the ensemble [27,30]. When a photon is stored in the ensemble, an atom changes from state $|a\rangle$ to $|d\rangle$. In state $|d\rangle$, the atom acts as a two-level atom that is resonant with the incident photon [see Fig. 1(a)]. Since the effective interaction is enhanced by the cavitylike behavior of the ensemble, this single two-level atom can make the entire ensemble become reflective instead of transmissive.

We focus on the behavior at the resonance nearest $\delta = 0$ (vertical dotted line in Fig. 2). In the limit of large atom number N and for $|\Delta_c| \neq 0$, this resonance is at a two-photon detuning $\delta_{\rm res} \approx -4\pi^2\Delta_c|\Omega_0|^2/(\Gamma_{\rm 1D}^2 N^2)$ for which we obtain [37]

$$r_0 \approx \frac{\Gamma_{\rm 1D}\Gamma' N}{16\Delta_c^2}, \tag{1}$$

$$t_0 \approx 1 - r_0, \tag{2}$$

$$r_1(\tilde{z}) \approx 1 - \frac{4\pi^2\Delta_c^2\Gamma'}{\Gamma_{\rm 1D}^3 N^2} - \frac{4i\pi^2\Delta_c}{\Gamma_{\rm 1D} N}\left(\tilde{z} - \frac{1}{2}\right) - \frac{4\pi^4\Delta_c^2(2\Gamma_{\rm 1D} + \Gamma')}{\Gamma_{\rm 1D}^3 N^2}\left(\tilde{z} - \frac{1}{2}\right)^2, \tag{3}$$

$$t_1(\tilde{z}) \approx \frac{4\pi^2\Delta_c^2\Gamma'}{\Gamma_{\rm 1D}^3 N^2} + \frac{8\pi^4\Delta_c^2\Gamma'}{\Gamma_{\rm 1D}^3 N^3}\left(\tilde{z} - \frac{1}{2}\right) + \frac{4\pi^4\Delta_c^2\Gamma'}{\Gamma_{\rm 1D}^3 N^2}\left(\tilde{z} - \frac{1}{2}\right)^2. \tag{4}$$

Here, t_1 and r_1 were obtained by solving the discrete problem where a photon is stored in a single discrete atom, and then taking the continuum limit such that the index of the atom is replaced by its position inside the ensemble $\tilde{z} = z/L$. By aligning the interferometer, the reflection coefficients of the combined interferometer-ensemble system are given by $R_0 = -(r_0 - t_0)$ and $R_1(\tilde{z}) = -[r_1(\tilde{z}) - t_1(\tilde{z})]$ [37]. If we take $\tilde{z} = 1/2$ and a detuning $|\Delta_c| \sim \Gamma_{\rm 1D} N^{3/4}$, we have r_0, $t_1 \sim \Gamma'/(\Gamma_{\rm 1D}\sqrt{N})$, $r_1 \approx 1 - t_1$, and $t_0 \approx 1 - r_0$. Hence, even for small $\Gamma_{\rm 1D}/\Gamma'$, we can achieve an ideal CPHASE gate ($R_0 = 1$, $R_1 = -1$) with sufficiently many atoms.

Fidelity.—To quantify the errors of the gate, we calculate the Choi-Jamiolkowski (CJ) fidelity [18,45]. The EIT storage is described using the storage K_s and retrieval K_r kernels derived in Ref. [33] (suitably modified to take into account storage from both directions [37]). When photon A is stored and retrieved without scattering of photon B, the output wave function of photon A is $\phi_{A,\rm out,0}(t) = \iint K_r(\tilde{z}, t)K_s(\tilde{z}, t')\phi_{A,\rm in}(t')dt'd\tilde{z}$, where $\phi_{A,\rm in}$ is the input wave function. The efficiency of the storage and retrieval is $\eta_{\rm EIT} = \int |\phi_{A,\rm out,0}(t)|^2 dt$. If photon B was reflected from the interferometer while photon A was stored in the ensemble (state $|11\rangle_{AB}$), the output wave function is instead $\phi_{A,\rm out,1}(t) = \iint K_r(\tilde{z}, t)R_1(\tilde{z})K_s(\tilde{z}, t')\phi_{A,\rm in}(t')dt'd\tilde{z}$. Neglecting bandwidth effects of photon B to find the upper limit set by the atomic ensemble, we obtain the CJ fidelity [45–47]

$$F_{\rm CJ} = \frac{\eta_{\rm EIT}}{16}|2t_b + R_0 - R_{1,1}|^2, \tag{5}$$

where $R_{1,1} = (1/\eta_{\rm EIT})\int \phi^*_{A,\rm out,0}(t)\phi_{A,\rm out,1}(t)dt$. If the gate is conditioned on the presence of two photons after the gate operation [18,48,49], we find the success probability

$$P_{\rm suc} = \frac{\eta_{\rm EIT}}{4}(2|t_b|^2 + |R_0|^2 + R_{1,2}), \tag{6}$$

with $R_{1,2} = (1/\eta_{\rm EIT})\int |\phi_{A,\rm out,1}(t)|^2 dt$. The conditional CJ fidelity is $F_{\rm CJ,cond} = F_{\rm CJ}/P_{\rm suc}$.

To optimize the performance of the gate, we set $t_b = 1$ and optimize Δ_c and the width of the stored spin wave $\tilde{\sigma} = \sigma/L$ such that $F_{\rm CJ}$ is maximal. In Fig. 3 we plot the numerically calculated $F_{\rm CJ} \approx P_{\rm suc}$ and $F_{\rm CJ,cond}$, where photon A was chosen to have a Gaussian temporal profile, and photon B is centered on $\delta = \delta_{\rm res}$ and assumed to be narrow in frequency compared to the resonance width. As seen in the figure, both $F_{\rm CJ}$ and $F_{\rm CJ,cond}$ approach their ideal value of unity for large N, but $F_{\rm CJ,cond}$ approaches it much faster.

For large N, we can find analytical expressions for the Λ-type curves in Fig. 3 if we neglect distortions of photon A under storage and retrieval, but still account for the errors due to the spatial extent of the stored excitation. The stored spin wave is approximately Gaussian of the form $S(\tilde{z}) = (2\pi\tilde{\sigma}^2)^{-1/4}\exp[-(\tilde{z} - 1/2)^2/(4\tilde{\sigma}^2)]$. Consequently, $\eta_{\rm EIT} \approx 1 - \Gamma'/(2N\Gamma_{\rm 1D}\tilde{\sigma}^2)$ [37,50], $R_{1,1} \approx \int R_{1,s}(\tilde{z})|S(\tilde{z})|^2 d\tilde{z}$, and $R_{1,2} \approx \int |R_{1,s}(\tilde{z})|^2|S(\tilde{z})|^2 d\tilde{z}$. Here, $R_{1,s}(\tilde{z}) = [R_1(\tilde{z}) + R_1(1 - \tilde{z})]/2$ is the symmetrized version of R_1 that accounts for storage and scattering from both sides of the ensemble.

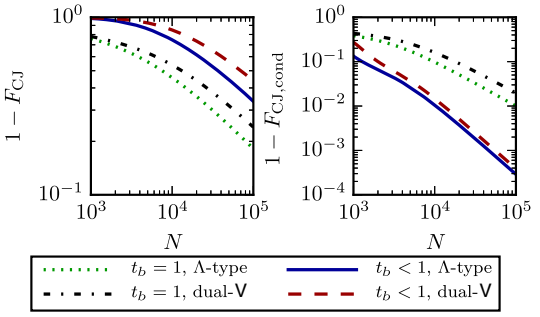

FIG. 3. Numerically calculated $F_{\rm CJ}$ and $F_{\rm CJ,cond}$. For the $t_b < 1$ curves, t_b is optimized numerically such that $F_{\rm CJ,cond}$ is maximal. The dual-V scheme uses regular interatomic distance $d = 0.266\pi/k_0$. The common parameters are $\Gamma_{\rm 1D}/\Gamma = 0.05$, and $\Omega_0/\Gamma = 1$. Under EIT (storage and retrieval), $\Omega(z) = \Omega_0$. Under stationary light (scattering), $\Omega(z) = \Omega_0\cos(k_0 z)$ and $\Omega_\pm(z) = \Omega_0 e^{\pm ik_0 z}$ for Λ-type and dual-V, respectively.

For fixed Γ_{1D} and large N, after choosing $\tilde{\sigma}^2 = 1/(\pi^{3/2}N^{1/4})\sqrt{\Gamma'/(\Gamma_{1D}+\Gamma')}$, $\Delta_c^2 = (\Gamma_{1D}^2 N^{3/2})/(8\pi)$, and $t_b = 1$, F_{CJ} is maximal, and

$$F_{CJ,t_b=1} \approx P_{suc,t_b=1} \approx 1 - \frac{\pi\Gamma'}{\Gamma_{1D}\sqrt{N}}, \tag{7}$$

$$F_{CJ,cond,t_b=1} \approx 1 - \frac{\pi^2\Gamma'^2}{4\Gamma_{1D}^2 N}. \tag{8}$$

These expressions confirm that the gate fidelity improves with N and that the conditional fidelity has better scaling.

With $t_b = 1$, the losses are different for the different computational basis states. By setting $t_b \approx R_0$ we approximately equalize the losses, leading to a substantial improvement of $F_{CJ,cond}$ at the cost of increasing $1 - P_{suc}$ by a constant factor. Whether this is a desirable trade off, depends on the particular application. Taking the same values of Δ_c and $\tilde{\sigma}$,

$$F_{CJ,t_b=R_0} \approx P_{suc,t_b=R_0} \approx 1 - \frac{2\pi\Gamma'}{\Gamma_{1D}\sqrt{N}}, \tag{9}$$

$$F_{CJ,cond,t_b=R_0} \approx 1 - \frac{11\pi^3(\Gamma_{1D}+\Gamma')\Gamma'}{16\Gamma_{1D}^2 N^{3/2}}. \tag{10}$$

Here, $1 - F_{CJ,cond}$ is limited by the nonzero $\tilde{\sigma}$.

Numerical simulations suggest that the fidelities are independent of Ω_0 over a wide range of values. For example, for $\Gamma_{1D}/\Gamma = 0.05$ and $N = 10^4$, $|\Omega_0|$ can be up to 30Γ with a negligible change in the optimal Δ_c, and up to at least 100Γ with some increase in the optimal Δ_c [37].

Dual-V scheme.—First, some technical differences from the Λ-type scheme. The decay rate Γ_{1D} is from each of the states $|b_\pm\rangle$ and $|e_\pm\rangle$ [see Fig. 1(b)]. When switched to state $|d\rangle$, the atom becomes a resonant V-type atom. For storage and retrieval, the Λ-type and dual-V schemes behave the same, since only one classical drive is incident. For the numerical calculation of the fidelities for the dual-V scheme in Fig. 3, the distance d between the atoms was set to be incommensurate with the wavelength of the classical drive, $d = 0.266\pi/k_0$. The results are, however, almost independent of d, and the gate can function even with completely random placement of the atoms [37]. The dual-V scheme is seen to have the same scaling as the Λ-type scheme.

Gate time.—The total gate time is split between EIT storage and retrieval, two π pulses, and scattering. The EIT time t_{EIT} is equal to the time to pass the ensemble, i.e., $t_{EIT} \sim L/v_g$, where $v_g = (2L|\Omega_0|^2)/(N\Gamma_{1D})$ is the EIT group velocity [50]. The π-pulse time t_π is set by the splitting between states $|a\rangle$ and $|d\rangle$. In the Supplemental Material [37], we discuss a specific implementation in ^{87}Rb where that splitting is proportional to Δ_c, resulting in $t_\pi \gtrsim 1/|\Delta_c|$.

To discuss scattering time, we need to model a nonzero bandwidth of photon B. The reflection coefficient R_0 (at $\delta = \delta_{res}$) in Eq. (5) should be replaced by $\int R_0(\delta)|\phi_B(\delta)|^2 d\delta$, where ϕ_B is the frequency distribution of photon B. Since r_1 and t_1 vary much slower than r_0 and t_0 around $\delta = \delta_{res}$ (see Fig. 2), we ignore a similar modification to $R_{1,1}$. By expanding, we get $r_0(\delta) \approx r_0(\delta_{res}) + (2/w^2)(\delta - \delta_{res})^2$ with the resonance width $w = (32\sqrt{2}\pi^2\Delta_c^2|\Omega_0|^2)/(\Gamma_{1D}^3 N^3)$. Defining $\sigma_B^2 = \int(\delta - \delta_{res})^2|\phi_B(\delta)|^2 d\delta$ (spectral width of photon B) and using the optimal $\Delta_c^2 = (\Gamma_{1D}^2 N^{3/2})/(8\pi)$, this gives a modification of the fidelity $F_{CJ,t_b=1,\sigma_B} \approx F_{CJ,t_b=1} - (\Gamma_{1D}^2 N^3 \sigma_B^2)/(16|\Omega_0|^4\pi^2)$. Requiring the error from nonzero σ_B to be the same as the error in Eq. (7), we find that the scattering time is $1/\sigma_B = (\Gamma_{1D}^{3/2} N^{7/4})/(4\pi^{3/2}\sqrt{\Gamma'}|\Omega_0|^2)$.

For $\Gamma_{1D}/\Gamma = 0.05$, $N = 10^4$, $|\Omega_0|/\Gamma = 10$, we have $t_{EIT} \sim 5/\Gamma$, $t_\pi \gtrsim 1/|\Delta_c| = 0.1/\Gamma$, and $1/\sigma_B \sim 52/\Gamma$. Hence, the scattering time is dominant in the total gate time ($\sim 1.6\ \mu$s for ^{87}Rb [51]). This is short compared to the coherence time expected for cooled and trapped atoms (e.g., few hundreds of microseconds in Ref. [52]).

Other imperfections.—Classical drives may couple states $|a\rangle$ and $|d\rangle$ off-resonantly to the excited states. The coupling of the former results in four-wave mixing noise, but this can be suppressed by a careful choice of the energy levels [37,53]. The coupling of the latter introduces loss of the stored photon with the effective rate $\Gamma_{eff} \sim \Gamma'|\Omega_0|^2/\Delta_{hfs}^2$ [37,54], where Δ_{hfs} is the hyperfine splitting of the ground states ($|a\rangle$ and $|c\rangle$). Hence, the total reduction in success probability during scattering is $\Gamma_{eff}/\sigma_B \sim (\Gamma_{1D}^{3/2}\sqrt{\Gamma'}N^{7/4})/(4\pi^{3/2}\Delta_{hfs}^2)$. For example, in ^{87}Rb, $\Delta_{hfs}/\Gamma \sim 10^3$ [51], and this error is negligible compared to other losses for $\Gamma_{1D}/\Gamma = 0.05$ and $N = 10^4$ but becomes significant for $N \sim 10^5$.

If the path lengths of the Sagnac interferometer are not completely stabilized, there is an additional error $\sim(k_0 l)^2$, where l is the deviation of the propagation length from the beam splitter to either end of the ensembles due to misalignment [37]. Finally, the heralded gate is rather insensitive to imperfections in the π pulses. The conditional fidelity will only be affected by the part of the excitation that still remains in states $|c\rangle$ after both π pulses and is subsequently read out with a wrong phase. This error thus only enters to a higher order and can be eliminated completely by doing EIT retrieval before the second π pulse [37].

Conclusion.—We have shown, how stationary light can be used to create a CPHASE gate between photons. Most importantly, the gate uses a large number of atoms N to compensate for a limited single-atom coupling to light. In particular, the gate can have a rapid convergence as $N^{-3/2}$ towards unit fidelity if it is operated in a heralded fashion. The gate is ideally suited for the setups currently under development [21–26], where there is a moderate coupling efficiency to light $\Gamma_{1D}/\Gamma \sim 10^{-3}$–$10^{-1}$ and total number of

atoms $N \sim 10^3$–10^5. In the Supplemental Material [37], we describe how the gate can be directly employed to improve the communication rate of quantum repeaters based on atomic ensembles. In general, the gate may serve as a tool for photonics based quantum information processing.

The research leading to these results was funded by the European Union Seventh Framework Programme through SIQS (Grant No. 600645) and ERC Grant QIOS (Grant No. 306576). J. B. acknowledges funding from the Carlsberg foundation.

Note added.—Recently, we became aware of a related study [55].

[1] H. J. Kimble, Nature (London) **453**, 1023 (2008).
[2] L.-M. Duan and H. J. Kimble, Phys. Rev. Lett. **92**, 127902 (2004).
[3] D. E. Chang, A. S. Sørensen, E. A. Demler, and M. D. Lukin, Nat. Phys. **3**, 807 (2007).
[4] H. Kim, R. Bose, T. C. Shen, G. S. Solomon, and E. Waks, Nat. Photonics **7**, 373 (2013).
[5] W. Chen, K. M. Beck, R. Bücker, M. Gullans, M. D. Lukin, H. Tanji-Suzuki, and V. Vuletić, Science **341**, 768 (2013).
[6] T. G. Tiecke, J. D. Thompson, N. P. de Leon, L. R. Liu, V. Vuletić, and M. D. Lukin, Nature (London) **508**, 241 (2014).
[7] B. Hacker, S. Welte, G. Rempe, and S. Ritter, Nature (London) **536**, 193 (2016).
[8] J. Volz, M. Scheucher, C. Junge, and A. Rauschenbeutel, Nat. Photonics **8**, 965 (2014).
[9] A. V. Akimov, A. Mukherjee, C. L. Yu, D. E. Chang, A. S. Zibrov, P. R. Hemmer, H. Park, and M. D. Lukin, Nature (London) **450**, 402 (2007).
[10] J. Claudon, J. Bleuse, N. S. Malik, M. Bazin, P. Jaffrennou, N. Gregersen, C. Sauvan, P. Lalanne, and J.-M. Gérard, Nat. Photonics **4**, 174 (2010).
[11] A. Goban, C.-L. Hung, S.-P. Yu, J. D. Hood, J. A. Muniz, J. H. Lee, M. J. Martin, A. C. McClung, K. S. Choi, D. E. Chang, O. Painter, and H. J. Kimble, Nat. Commun. **5**, 3808 (2014).
[12] I. Söllner, S. Mahmoodian, S. L. Hansen, L. Midolo, A. Javadi, G. Kiršanskė, T. Pregnolato, H. El-Ella, E. H. Lee, J. D. Song, S. Stobbe, and P. Lodahl, Nat. Nanotechnol. **10**, 775 (2015).
[13] K. Hammerer, A. S. Sørensen, and E. S. Polzik, Rev. Mod. Phys. **82**, 1041 (2010).
[14] M. Saffman, T. G. Walker, and K. Mølmer, Rev. Mod. Phys. **82**, 2313 (2010).
[15] D. Roy, C. M. Wilson, and O. Firstenberg, Rev. Mod. Phys. **89**, 021001 (2017).
[16] A. V. Gorshkov, J. Otterbach, M. Fleischhauer, T. Pohl, and M. D. Lukin, Phys. Rev. Lett. **107**, 133602 (2011).
[17] M. Khazali, K. Heshami, and C. Simon, Phys. Rev. A **91**, 030301 (2015).
[18] S. Das, A. Grankin, I. Iakoupov, E. Brion, J. Borregaard, R. Boddeda, I. Usmani, A. Ourjoumtsev, P. Grangier, and A. S. Sørensen, Phys. Rev. A **93**, 040303 (2016).
[19] C. R. Murray and T. Pohl, Phys. Rev. X **7**, 031007 (2017).
[20] F. Le Kien, V. I. Balykin, and K. Hakuta, Phys. Rev. A **70**, 063403 (2004).
[21] E. Vetsch, D. Reitz, G. Sagué, R. Schmidt, S. T. Dawkins, and A. Rauschenbeutel, Phys. Rev. Lett. **104**, 203603 (2010).
[22] A. Goban, K. S. Choi, D. J. Alton, D. Ding, C. Lacroûte, M. Pototschnig, T. Thiele, N. P. Stern, and H. J. Kimble, Phys. Rev. Lett. **109**, 033603 (2012).
[23] J.-B. Béguin, E. M. Bookjans, S. L. Christensen, H. L. Sørensen, J. H. Müller, E. S. Polzik, and J. Appel, Phys. Rev. Lett. **113**, 263603 (2014).
[24] B. Gouraud, D. Maxein, A. Nicolas, O. Morin, and J. Laurat, Phys. Rev. Lett. **114**, 180503 (2015).
[25] M. Bajcsy, S. Hofferberth, V. Balic, T. Peyronel, M. Hafezi, A. S. Zibrov, V. Vuletic, and M. D. Lukin, Phys. Rev. Lett. **102**, 203902 (2009).
[26] F. Blatt, L. S. Simeonov, T. Halfmann, and T. Peters, Phys. Rev. A **94**, 043833 (2016).
[27] M. Hafezi, D. E. Chang, V. Gritsev, E. Demler, and M. D. Lukin, Phys. Rev. A **85**, 013822 (2012).
[28] A. André and M. D. Lukin, Phys. Rev. Lett. **89**, 143602 (2002).
[29] M. Bajcsy, A. S. Zibrov, and M. D. Lukin, Nature (London) **426**, 638 (2003).
[30] I. Iakoupov, J. R. Ott, D. E. Chang, and A. S. Sørensen, Phys. Rev. A **94**, 053824 (2016).
[31] F. E. Zimmer, J. Otterbach, R. G. Unanyan, B. W. Shore, and M. Fleischhauer, Phys. Rev. A **77**, 063823 (2008).
[32] S. A. Moiseev and B. S. Ham, Phys. Rev. A **73**, 033812 (2006).
[33] A. V. Gorshkov, A. André, M. D. Lukin, and A. S. Sørensen, Phys. Rev. A **76**, 033805 (2007).
[34] G. Bertocchi, O. Alibart, D. B. Ostrowsky, S. Tanzilli, and P. Baldi, J. Phys. B **39**, 1011 (2006).
[35] M. Bradford, K. C. Obi, and J.-T. Shen, Phys. Rev. Lett. **108**, 103902 (2012).
[36] I. H. Deutsch, R. J. C. Spreeuw, S. L. Rolston, and W. D. Phillips, Phys. Rev. A **52**, 1394 (1995).
[37] See Supplemental Material at http://link.aps.org/supplemental/10.1103/PhysRevLett.120.010502 for further details. It additionally uses Refs. [38–44].
[38] L.-M. Duan, M. D. Lukin, J. I. Cirac, and P. Zoller, Nature (London) **414**, 413 (2001).
[39] N. Sangouard, C. Simon, H. de Riedmatten, and N. Gisin, Rev. Mod. Phys. **83**, 33 (2011).
[40] N. Sangouard, C. Simon, B. Zhao, Y.-A. Chen, H. de Riedmatten, J.-W. Pan, and N. Gisin, Phys. Rev. A **77**, 062301 (2008).
[41] J. Borregaard, P. Kómár, E. M. Kessler, M. D. Lukin, and A. S. Sørensen, Phys. Rev. A **92**, 012307 (2015).
[42] T. Peters, Y.-H. Chen, J.-S. Wang, Y.-W. Lin, and I. A. Yu, Opt. Lett. **35**, 151 (2010).
[43] I. Vurgaftman and M. Bashkansky, Phys. Rev. A **87**, 063836 (2013).
[44] T. Caneva, M. T. Manzoni, T. Shi, J. S. Douglas, J. I. Cirac, and D. E. Chang, New J. Phys. **17**, 113001 (2015).
[45] A. Gilchrist, N. K. Langford, and M. A. Nielsen, Phys. Rev. A **71**, 062310 (2005).
[46] I. Iakoupov, Ph.D. thesis, University of Copenhagen, 2016.
[47] I. Iakoupov and A. S. Sørensen (to be published).

[48] L.-M. Duan, B. Wang, and H. J. Kimble, Phys. Rev. A **72**, 032333 (2005).
[49] J. Borregaard, P. Kómár, E. M. Kessler, A. S. Sørensen, and M. D. Lukin, Phys. Rev. Lett. **114**, 110502 (2015).
[50] D. E. Chang, A. H. Safavi-Naeini, M. Hafezi, and O. Painter, New J. Phys. **13**, 023003 (2011).
[51] D. A. Steck, Rubidium 87 D Line Data, available online at http://steck.us/alkalidata (revision 2.1.5, 2015).
[52] J.-B. Béguin, J. H. Müller, J. Appel, and E. S. Polzik, arXiv:1708.08387.
[53] P. Walther, M. D. Eisaman, A. André, F. Massou, M. Fleischhauer, A. S. Zibrov, and M. D. Lukin, Int. J. Quantum. Inform. **05**, 51 (2007).
[54] F. Reiter and A. S. Sørensen, Phys. Rev. A **85**, 032111 (2012).
[55] O. Lahad and O. Firstenberg, Phys. Rev. Lett. **119**, 113601 (2017).